Supporting Information

Functionalized Gold Nanorod Solution via Reverse Micelle based Polyacrylate Coating

*SK Basiruddin, Arindam Saha, Narayan Pradhan, and Nikhil R. Jana**

Centre for Advanced Materials, Indian Association for the Cultivation of Science, Kolkata-700032, India

**Corresponding authors. E-mail: camnrj@iacs.res.in*

Methods for the calculation of quantum yield for nanorod-fluorescein: We used the equation $(QY)_{Sm} = (QY)_{St} \times [(PL\ area/OD)_{Sm}/(PL\ area/OD)_{St}]$, for QY calculation where S_m stands for sample and S_t stands for standard, PL area is the area under the fluorescence spectrum and OD is the absorbance. Here fluorescein-o-methacrylate was used as standard (assuming its QY is similar to fluorescein) with QY of 95%. All fluorescence spectra for QY calculation were obtained by exciting at 475 nm.

The absorbance contribution of fluorescein in composite system was calculated from UV-visible spectra shown in Figure S1. Fluorescein showed strong absorbance peak at ~ 500 nm in basic medium but it became weak in acidic medium. Thus absorption spectrum of nanorod-fluorescein shows a strong peak at ~ 500 nm in basic medium which has a contribution due to fluorescein and transverse plasmon band of nanorod. However, this band becomes weaker at acidic medium. The difference in absorbance at 500 nm for pH 5.0 and 9.0 was assumed as representative of fluorescein concentration. The QY calculated by this approach was ~9 %.

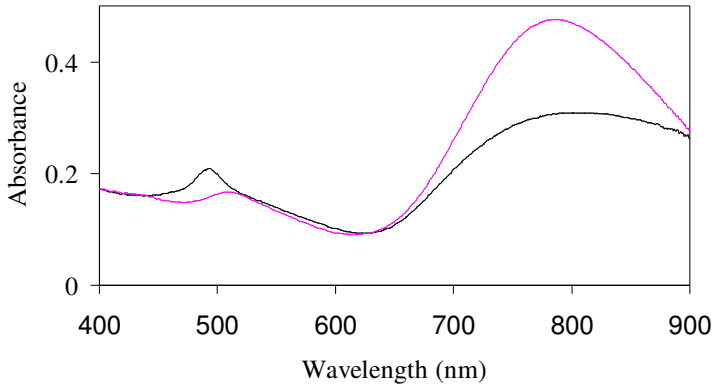

Figure S1. UV-visible spectra of nanorod-fluorescein solution at pH 5 (black) and pH 9 (pink). The difference in absorbance at 500 nm is mainly contributed by fluorescein (as it has pH dependent changes in absorbance) and this change has been used to determine its concentration. The absorbance change at 700-900 nm is due to pH dependent partial aggregation of nanorods.

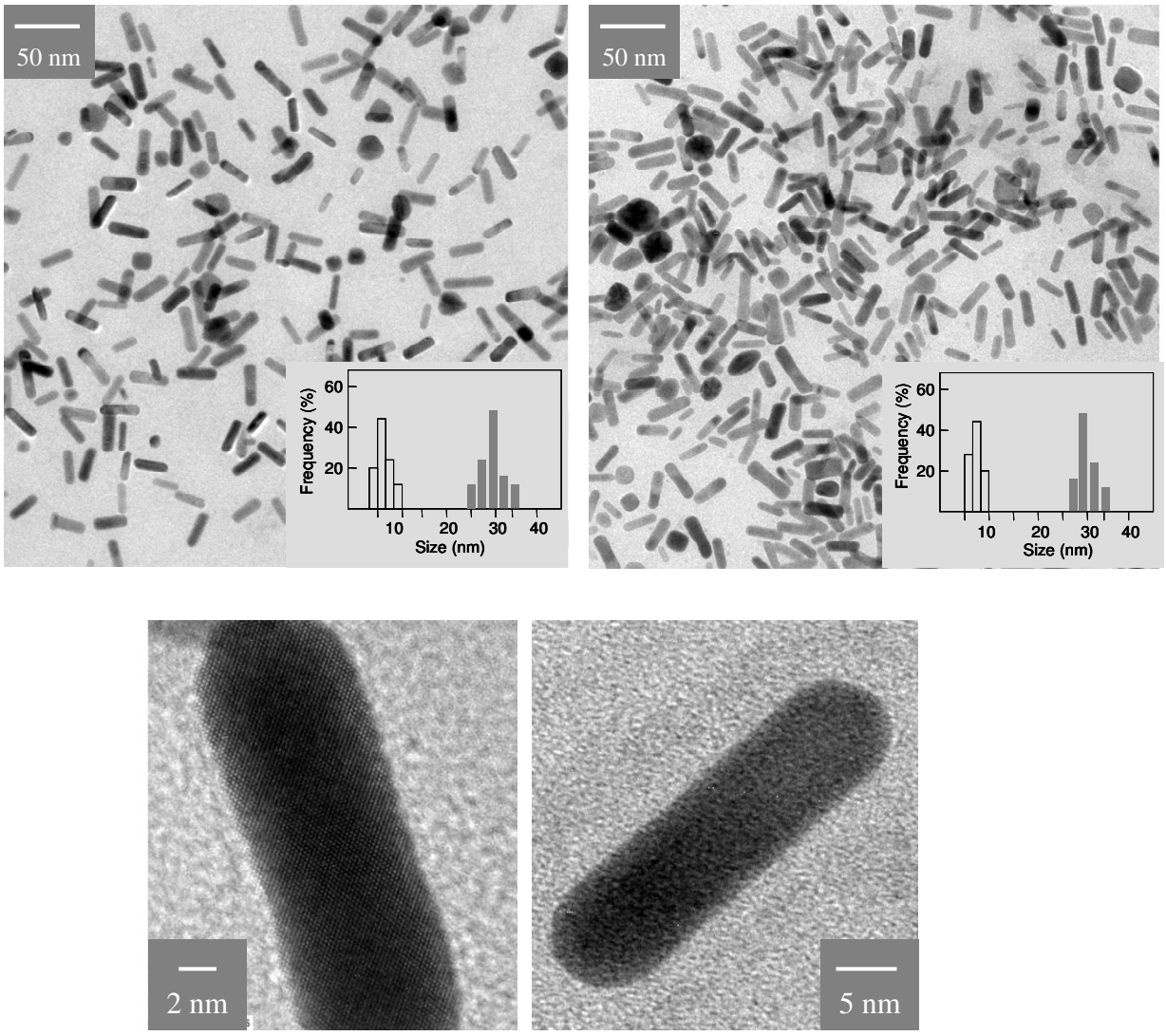

Figure S2. Top panel shows low resolution TEM images of as synthesized gold nanorods (left) and same batch of nanorods after polyacrylate coating (right). Inset shows histogram of their shape distribution. (□ short axis distribution, ■ long axis distribution)

Bottom panel shows the high resolution TEM image of thin polyacrylate (1 hr coating) coated nanorod (left), same sample after ammonium molybdate staining (right). It shows that thin polymer shell is invisible even after staining.

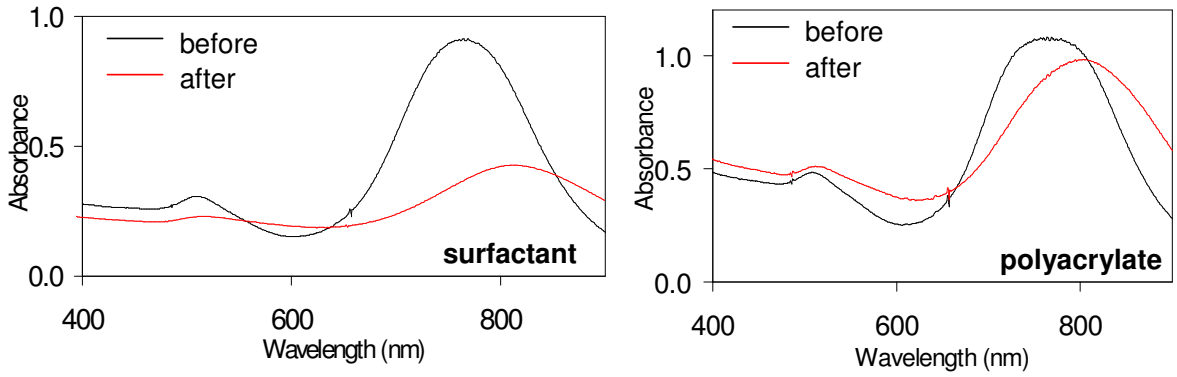

Figure S3. Colloidal stability of gold nanorod solutions after 6 hrs of dialysis --- as observed by UV-visible absorption spectral studies. It shows that surfactant capped as synthesized nanorods starts precipitating (as observed from lowering of plasmon absorbance) but polyacrylate coated nanorods do not show such precipitation but some peak shift possibly due to change of ionic strength.

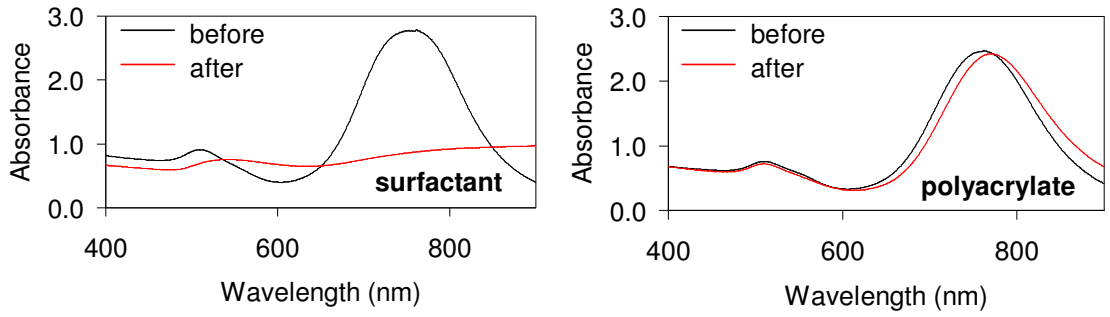

Figure S4. Colloidal stability of gold nanorod solutions in 1:2 volume percent ethanol-water medium, as observed through UV-visible absorption spectral studies. It shows that surfactant capped as synthesized nanorods precipitate (as observed from disappearance of plasmon absorbance) but polyacrylate coated nanorods do not show such precipitation.

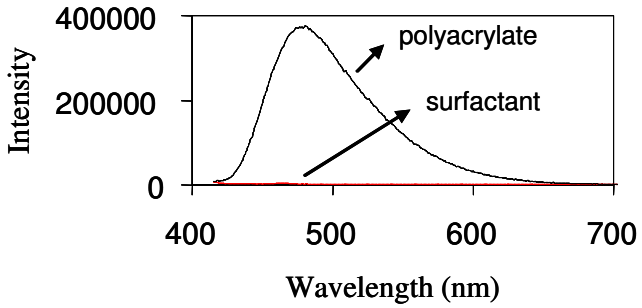

Figure S5. Fluorescamine test of polyacrylate coated gold nanorod solution showing that primary amines have been incorporated in coating backbone during the coating step.

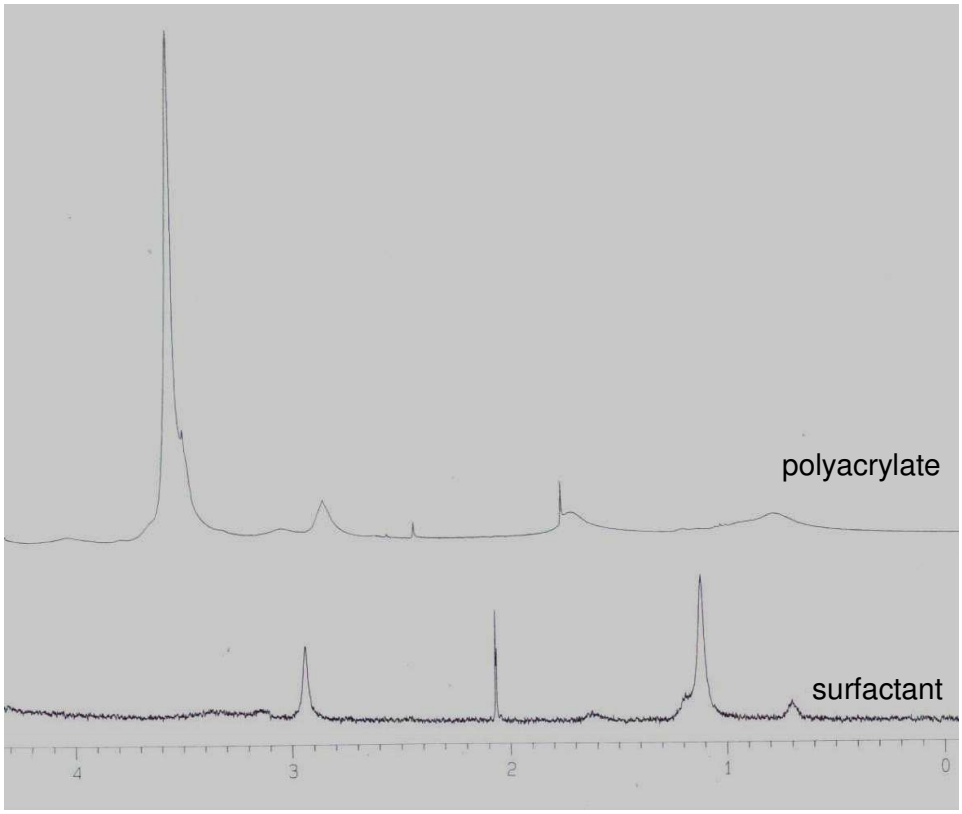

Figure S6. Proton NMR of surfactant stabilized and polyacrylate coated gold nanorods studied in D_2O. It shows that surfactants are replaced by polymer after coating. In surfactant capped nanorods, the bands at 0.5-1.5 ppm due to alkyl protons and at 2.8-3.2 ppm due to methyl/methylene groups of trimethyl ammonium ion of surfactant head. In polyacrylate coated nanorods, the broad bands at 0.5–3.8 ppm is due to the acrylate polymer and weaker broad band at 3.9–4.1 is attributed to the methylene group of methylenebisacrylamide.

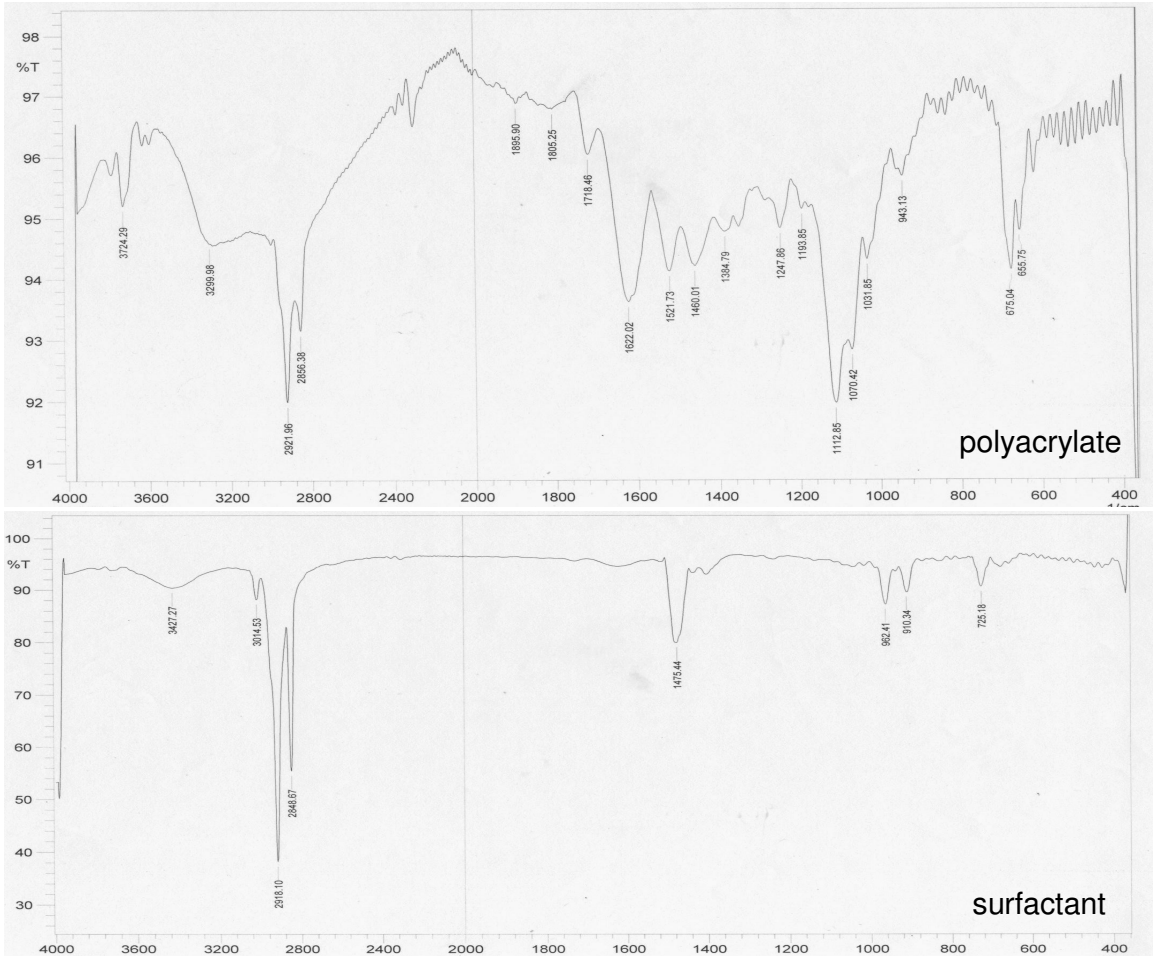

Figure S7. FTIR spectra of surfactant stabilized and polyacrylate coated gold nanorods. Surfactant capped nanorods show strong peaks at 2918 cm^{-1} and 2848 cm^{-1}due to stretching vibrations of CH_3 and CH_2 coming from surfactants. After polymer coating those peaks became weaker with the appearance of new peaks particularly at 1000-1700 cm^{-1} region. The peak at 3299 cm^{-1}due to PEG alcohol groups, peaks at 2921 cm^{-1} and 2856 cm^{-1} are due to methyl / methylene groups, peaks at 1622 cm^{-1}, 1521 cm^{-1}, 1460 cm^{-1} are due to carbonyl and primary amine groups.

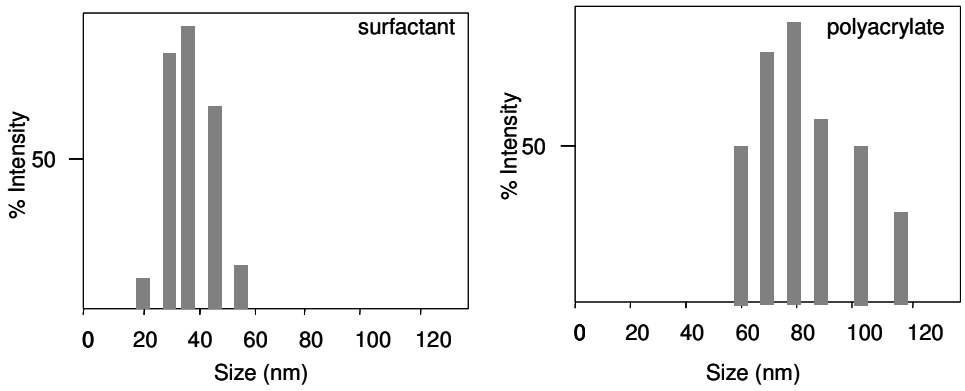

Figure S8. Particle size distribution data of gold nanorod solution before and after polyacrylate coating as observed from dynamic light scattering (DLS) study.

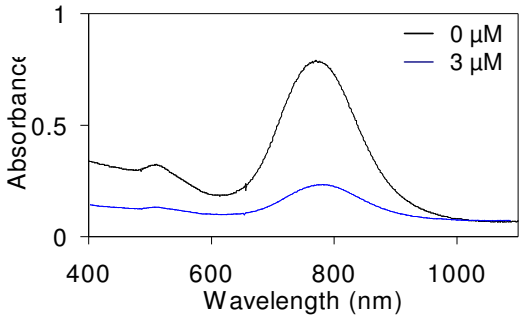

Figure S9. Biochemical activity test of biotin functionalized gold nanorods. The absorption spectra of biotin functionalized gold nanorods (black) and supernatant of same solution after addition of Streptavidin (blue). Nanorods aggregate and precipitate from solution upon addition of Streptavidin as it has four glucose binding sites that induce cross-linking of nanorods.

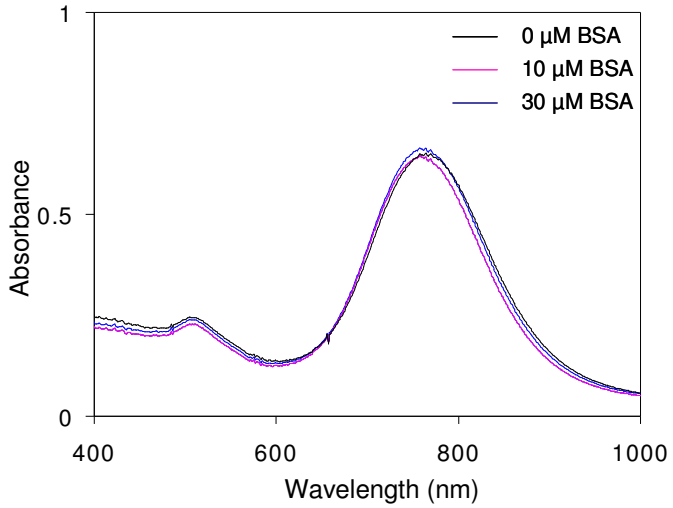

Figure S10. Control BSA test of glucose functionalized gold nanorods. Nanorods do not aggregate upon addition of BSA as indicated from unchanged absorption spectra. This result indicates minimum non-specific interaction of functional nanorods.